EMITTANCE MEASUREMENT USING X-RAY LENSES AT THE ESRF

F. Ewald, J.-C. Biasci, L. Farvacque, K.-B. Scheidt, ESRF, Grenoble, France

Abstract

During 2011, X-ray lenses were tested as an alternative way of emittance measurement in the ESRF storage ring [1]. Following these tests it was decided to install a new bending magnet diagnostic beam port dedicated primarily to a permanent emittance measurement using X-ray lens imaging. The new beam port is equipped with a thin (0.6 mm) double CVD diamond window instead of 3 mm aluminium used at the pinhole beam ports. This increases the X-ray transmission, especially at low energies. The imaging and emittance measurement using aluminium lenses is discussed in comparison to the emittance measurement based on pinhole imaging. Although the principle works correctly, the setup presents different practical difficulties, such as low signal intensity and heat load.

NEW DIAGNOSTICS BEAM PORT D11

The new diagnostic beam port is located behind the second dipole of cell 11. The second dipole of each storage ring cell has a 0.4 T field at its entrance. The 0.86 T field is reached at about $s = 300$ mm from the ideal entrance in the dipole field, corresponding to an angle of X-ray emission of about -6 mrad. We decided to use the 0.86 T field for its high photon flux and energies. A modified beam port absorber allows to extract 0.35 mrad of the dipole radiation at a center angle of -11.9 mrad. In contrast to the two existing diagnostics beam ports D9 and ID25, the beam port window is not made of aluminium, but of a CVD diamond window. This choice was made because it allows to work at much lower X-ray energies (even visible light) and secondly it reduces a possible influence of X-ray scattering from the window material on the beam quality. We use a double window as an additional security against venting of the storage ring in case of leaks. Each CVD window is only 300 μm thick with a diameter of about 4 mm. Both windows are water cooled.

The power radiated from a 0.86 T ESRF bending magnet at a nominal stored current of 200 mA is $P = 158$ W/mrad. The CVD windows ($= 0.6$ mm thickness) absorb mainly low energy X-rays, transmitting still 125 W/mrad. The power transmitted through the absorber opening is ≈ 44 W. This is a considerable power, that will be absorbed by any elements in the beam path, inducing heating, radiation damage and corrosion. Therefore, if needed, a wedge shaped copper attenuator can be inserted into the beam.

The second CVD window (vacuum-air interface) is continuously flushed with a N_2 flow, thus preventing corrosion of the copper parts of the window assembly. The lenses are mounted in a box with integrated nitrogen flow. The best solution to avoid ozone production between the window and the lenses is to keep the beam path as much oxygen free as possible. Since a setup in vacuum is complicated, the beam path between the CVD window and the lens has been confined within a bellow made of kapton foil (see Figure 1), the volume inside being filled with nitrogen via the flow through the lens box and the CVD window. Unfortunately, even with this simple protection considerable corrosion on the attenuator as well as in the whole vicinity of the setup is observed. A better solution for ozone confinement or reduction has to be found.

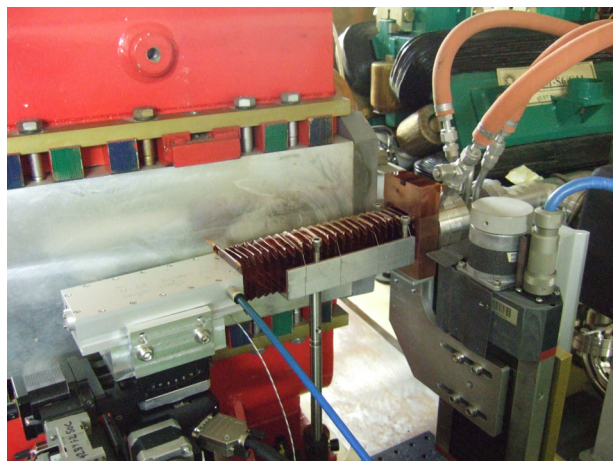

Figure 1: Implementation of the nitrogen purged lens (aluminium box on the left with blue N_2 tube). A Cu attenuator is installed at the CVD window exit (red tubes = water cooling). The kapton bellow flushed with nitrogen should reduce ozone production between the CVD window and the lens.

To get the highest photon flux possible for the emittance measurement, the Cu-attenuator is completely removed from the beam. Collimators (~ 2 cm brass) placed in front of the lens reduce the incident beam size to 500 μm in diameter. The power incident on the first lens is therefore about 14 W. For the peak energy of the incident X-ray spectrum about 6% will be absorbed in the first lens (see expression for transmission trough parabolic lenses in [2]. This corresponds to roughly 1 W. The following lenes will absorb less and less power. Thus the absorption is distributed over the first layers of lenses instead of taking place in the first lens only. A thermocouple measuring the temperature very close to the first lens measures temperatures reaching 95 °C at 200 mA stored current. This is an uncritical temperature concerning destruction or deformation of the Al-lens. Indeed, the lenses show no damage after a few months of exposure to the full beam ,

ISBN 978-3-95450-127-4

as has been verified by scanning electron microscopy of the first lens in the stack.

Emittance Setup

The main aim of the beam port D11 is the emittance measurement using X-ray imaging with lenses. The X-rays are imaged onto a scintillator screen (0.5 mm $CdWO_4$). The visible light emitted from the screen is then imaged with a double achromat to a CCD camera (see sketch in Figure 2. Downstream from the absorber the lenses are installed. The X-rays transmitted through the lenses are monochromatised with a Si crystal in Laue configuration (diffracting planes are the (111)-planes). The choice of

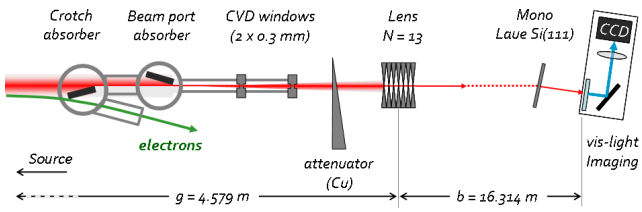

Figure 2: Setup for emittance measurement at beam port D11 (distances not to scale).

the number of lenses to be used is dictated by the magnification of the setup and by the maximum possible X-ray transmission through the lens stack, the vacuum window and the drift space in air. Therefore the optimum energy of the dipole spectrum which results in the highest flux after transmission has to be found. Figure 3 shows the transmitted flux as a function of the photon energy. The optimum energy is located around $31 - 32$ keV. A number of $N = 13$ lenses creates a sharp image for a photon energy of $E = 32$ keV. Figure 4 shows the energy scan (vertical beam size versus energy) used to experimentally confirm the best focusing at this optimum energy.

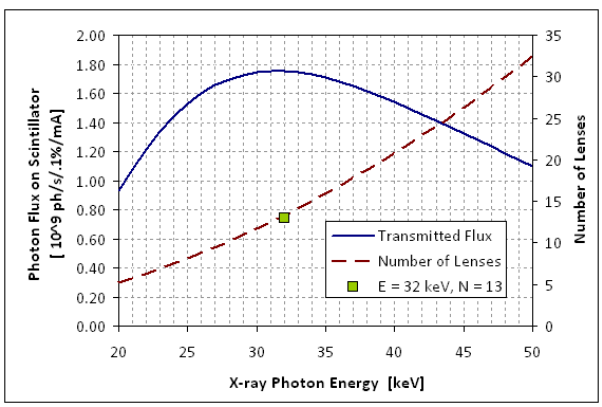

Figure 3: Simulated photon flux detected by the scintillator. For each X-ray energy, the number of lenses changes. The optimum is found for $E = 32$ keV and $N = 13$.

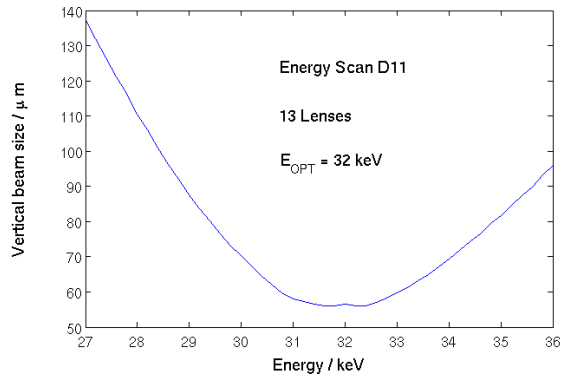

Figure 4: Scan of vertical beam size of the monochromatic beam as function of the X-ray energy. The optimum energy for which the focal distance fits with the object and image distances is 32 keV.

Source Position and Emittance Calculation

As for the pinhole setup, the emittance measurement requires the knowledge of the source-to-lens and source-to-detector distances as well as the lattice functions at the source. Therefore, first, the source point has to be determined correctly, then the lattice functions given at the ideal starting point of the bent trajectory have to be transported to the real source point. In the case of X-ray lenses the imaged spot is for experimental reasons the vertical waist of the X-ray beam and not the geometrical source point of the chosen emission angle on the electron trajectory, from where the observed X-rays are emitted. Waist position and geometrical source point are determined in the following as well as the expression for the electron beam emittance.

The phase-space ellipse of the electron beam at the ideal entrance point into the dipole is:

$$\Sigma_0 = \begin{pmatrix} \sigma_e^2 & -\varepsilon\alpha \\ -\varepsilon\alpha & \sigma'^2 \end{pmatrix} \quad , \tag{1}$$

with σ_e being the electron beam size at this position, σ' the divergence, ε the emittance, and α the usual lattice function. The X-ray source, however, is located at a distance $s = 435$ mm from this point 0, corresponding to the observation angle of -11.9 mrad.

The phase-space ellipse has therefore to be transported to this point s. In the present case we assume that the dipole is well represented by a drift space $T_s = \begin{pmatrix} 1 & s \\ 0 & 1 \end{pmatrix}$, knowing that focusing effects are negligible in our case due to the large bending radius. The phase-space ellipse Σ_s of the electron beam at the position s is:

$$\Sigma_s = T_s \Sigma_0 T_s^{\mathrm{T}} = \begin{pmatrix} \sigma_e^2 - 2s\varepsilon\alpha + s^2\sigma_e'^2 & s\sigma_e'^2 - \varepsilon\alpha \\ s\sigma_e'^2 - \varepsilon\alpha & \sigma_e'^2 \end{pmatrix} .$$

The electron beam size $\sigma_{e,s}$ at the position s is equal to $\sqrt{\Sigma(1,1)}$.

The X-rays detected by the lens imaging (or pinhole) setup

ISBN 978-3-95450-127-4

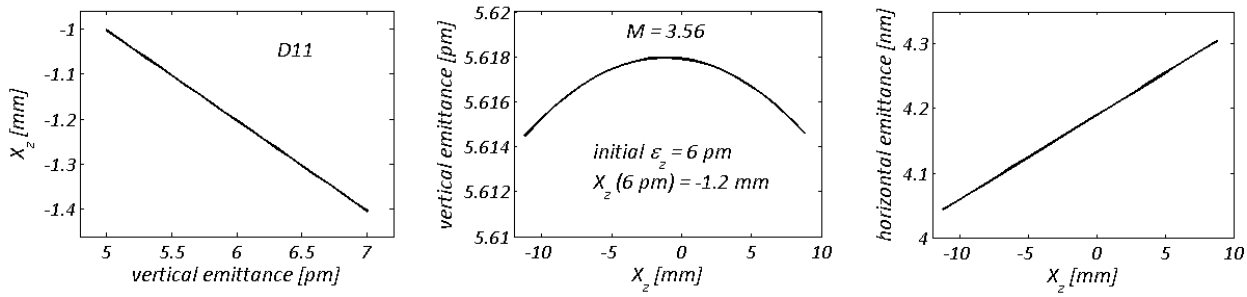

Figure 5: Left: Waist position X as function of the emittance in the case of the D11 beam port. The emittance values were chosen around a nominal emittance of 6 pm. The waist position changes very little with the emittance. Center and right: vertical and horizontal emittance scaling with X_{Z}. The emittances for different supposed waist positions X_{z} were calculated using a real measured beam size of 50 μm on the scintillator screen.

are originating from this point s. The phase-space ellipse of the photon beam at the position s is:

$$\Sigma_s^{\mathrm{ph}} = \begin{pmatrix} \sigma_{\mathrm{e,s}}^2 & s\sigma_{\mathrm{e}}'^2 - \varepsilon\alpha \\ s\sigma_{\mathrm{e}}'^2 - \varepsilon\alpha & \sigma_{\mathrm{T}}'^2 \end{pmatrix} \quad , \tag{2}$$

where σ_{T}' is the total X-ray beam divergence given by the convolution of electron and photon beam divergence:

$$\sigma_{\mathrm{T}}'^2 = \sigma_{\mathrm{e}}'^2 + \sigma_{\mathrm{ph}}'^2 \quad .$$

The natural intrinsic source beam size of synchrotron radiation being negligibly small, the photon beam size is equal to the electron beam size $\sigma_{\mathrm{e,s}}$.

Due to the extended electron beam size combined with the synchrotron radiation divergence, the virtual photon beam waist is not located at the point of photon emission. This effect can be calculated using the matrix representation of the phase-space ellipse of the emitted photon beam. In order to find the waist of the emitted synchrotron radiation beam, we translate Σ_s^{ph} by a distance X:

$$\Sigma_X^{\mathrm{ph}} = T_{\mathrm{X}} \begin{pmatrix} \sigma_{\mathrm{e,s}}^2 & s\sigma_{\mathrm{e}}'^2 - \varepsilon\alpha \\ s\sigma_{\mathrm{e}}'^2 - \varepsilon\alpha & \sigma_{\mathrm{T}}'^2 \end{pmatrix} T_{\mathrm{X}}^{\mathrm{T}} \quad . \tag{3}$$

At the waist position the phase-space ellipse is upright, which means that $\Sigma_X^{\mathrm{ph}}(1,2) \equiv 0$, from which X is calculated:

$$X = \frac{\varepsilon\alpha - s\sigma_{\mathrm{e}}'^2}{\sigma_{\mathrm{e}}'^2 + \sigma_{\mathrm{ph}}'^2(E_{\mathrm{ph}})} \quad . \tag{4}$$

In practice the alignment of the setup is done on minimisation of the vertical beam waist (see Figure 4). Since in the vertical plane η and η' are negligibly small, the vertical waist position is then:

$$X_{\mathrm{z}} = \frac{\alpha - s\gamma}{\gamma + \frac{1}{\varepsilon}\sigma_{\mathrm{ph}}'^2(E_{\mathrm{ph}})} \quad , \quad \gamma = (\frac{1+\alpha^2}{\beta}) \quad . \tag{5}$$

Using a typical emittance value of $\varepsilon = 6$ pm and the lattice parameters listed in Table 1 yields $X_{\mathrm{z}} = -1.2$ mm. Thus, the waist is located slightly upstream of the point $s = 435$ mm. It is this waist that is imaged by the lens when the energy is optimised for smallest spot size on the detector (see figure 4), while the source of X-rays is at the point s.

The beam spot size as detected with the CCD will be called Σ_{tot}. It contains a contribution σ_{opt}, describing the resolution of the visible light imaging system (screen resolution, abberations, pixel size). The X-ray source size is then

$$\sigma_{\mathrm{ph,X}}^2 = \frac{\Sigma_{\mathrm{tot}}^2 - \sigma_{\mathrm{opt}}^2}{M^2} \quad , \tag{6}$$

with M being the magnification of the X-ray lens imaging:

$$M = (D_{\mathrm{screen}} - D_{\mathrm{lens}})/(D_{\mathrm{lens}} - (s + X_{\mathrm{z}})) = 3.58 \tag{7}$$

From equation 3, and 2 we get

$$\begin{aligned} \sigma_{\mathrm{ph,X}}^2 \quad &= \quad \varepsilon(\beta - 2\alpha(s+X_{\mathrm{z}}) + \gamma(s+X_{\mathrm{z}})^2) \ldots \\ &+ \quad \eta_{(\mathrm{s+X_z})}^2\delta^2 + X_{\mathrm{z}}^2\sigma_{\mathrm{ph}}'^2 \quad , \end{aligned} \tag{8}$$

with δ being the electron energy spread and

$$\eta_{(\mathrm{s+X_z})} = \eta + \eta'(s+X_{\mathrm{z}}) + \rho\left(1 - cos\left(\frac{s+X_{\mathrm{z}}}{\rho}\right)\right) \tag{9}$$

the dispersion propagated to the position $(s+X_{\mathrm{z}})$ along the dipole field (ρ is the dipole bending radius, $\rho(0.86\ \mathrm{T}) = 23.49$ m, $\rho(0.4\ \mathrm{T}) = 49.76$ m). Therewith the electron beam emittance can be calculated from the lattice functions given at the point $s = 0$:

$$\varepsilon = \frac{\left[\frac{\Sigma_{\mathrm{tot}}^2 - \sigma_{\mathrm{opt}}^2}{M^2} - X_{\mathrm{z}}^2\sigma_{\mathrm{ph}}'^2 - \eta_{(\mathrm{s+X_z})}^2\delta^2\right]}{\beta - 2\alpha(s+X_{\mathrm{z}}) + \gamma(s+X_{\mathrm{z}})^2} \tag{10}$$

Obviously X_{z} is a function of the electron beam emittance itself (eq. 4). Therefore also the emittance calculated by eq. 10 is a function of itself. In the left plot of Figure 5 the quasi linear dependence of the waist position on the electron beam emittance is shown for the case of D11 (using eq. 5). The waist position is changing by less than 1 mm/pm with the emittance. In normal operation the vertical emittance does not vary by more than 2 or 3 pm and

ISBN 978-3-95450-127-4

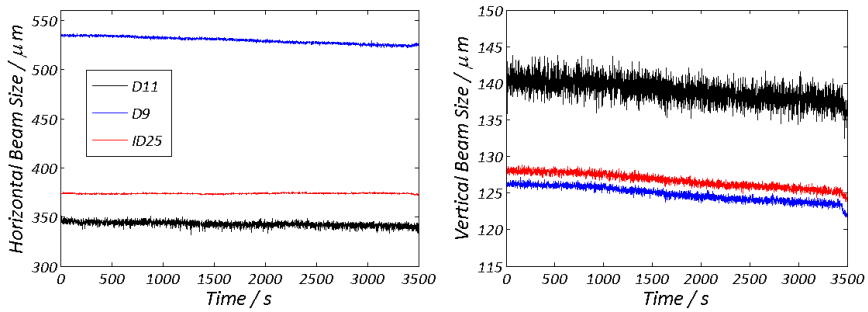

Figure 6: Horizontal and vertical beam sizes (σ) on the scintillator screen measured at the beam ports D11 (lens), D9 and ID25 (pinholes) during 16-bunch operation ($\sim$ 80 mA, large vertical emittance due to artificial beam blow up). The higher noise level of the D11 signal is obvious. (The decrease of beam sizes with time is due to the change of energy spread (horizontal plane) and the lower efficiency of the beam blow up at low bunch currents ($\propto$ time).

Table 1: Lattice Parameters and Distances of Pinhole, Lens and Scintillator Screen to the -11.9 mrad Source Point s.

β_x	=	2.5488 m	β_z	=	32.1388 m
α_x	=	1.5229 m	α_z	=	-0.2083 m
η_x	=	0.1 m	η_z	=	0 m
η'_x	=	-0.0734 m	η'_z	=	0 m
δ	=	0.00106			
$\sigma'_{ph}(32\ \mathrm{keV})$	=	33.29 μrad			
s	=	435 mm			
X_z	=	-1.2 mm			
$D_{pinhole}$	=	$(4363 - s)$ mm			
D_{lens}	=	$(4579 - s)$ mm			
D_{mono}	=	$(20677 - s)$ mm			
D_{screen}	=	$(20893 - s)$ mm			

a small change of X_z on the magnification and the lattice parameters is therefore small.

Using a first guessed value ε_{start}, X_z is determined and used in the calculation of the vertical emittance ε_z from the measured beam size using equation 10. Iterating in this way, the correct emittance is determined. Due to the weak dependence of X_z on ε_z the result converges already after the first iteration, and we decided to fix the first guessed emittance value ε_{start}, since a small change in X_z introduced by a varying ε_z is negligible. The center plot of Figure 5 illustrates this: in the expected range of variation of X_z the calculated emittance is not affected within our measured precision of about 0.1 pm in the vertical plane. In the horizontal plane (right plot) the influence is stronger but still within the precision of measurement of 0.1 nm.

In comparison with the pinhole cameras the image intensity is low (due to monochromatisation). The CCD camera is therefore always working close to its longest exposure time and highest gain. This increases the noise level of the signal significantly (see Figure 6). Additionally it reduces the tolerance versus ageing cameras (degrading linearity, increasing background level) and thus makes the lens setup less reliable at low beam currents compared to the pinhole systems. The analysis of the beam size fluctuation over time measured at D11 during 16-bunch filling (Figure 6) results in relative rms emittance fluctuations $\Delta\varepsilon/\varepsilon = 2\Delta\sigma/\sigma$ of $\sim 1\%$ in the horizontal and $\sim 2\%$ in the vertical plane. In comparison to $\sim 0.2\%$ (horizontal) and $\sim 0.4\%$ (vertical) for the pinholes D9 and ID25, the D11 setup performs clearly worse. The above data was taken during 16-bunch mode, i.e. not with the highest possible storage ring current and an artificial beam blow up (to increase the lifetime). This leads to a low image intensity and stronger noise as explained above. While at 200 mA stored current and low emittance the performance of the D11 device is good, it clearly looses precision at low electron beam current, as e.g. during 4-bunch mode or machine studies.

CONCLUSIONS

The D11 lens system for emittance measurement has been operating continuously for about 9 month (since January 2013). At the present status the results are not fully satisfactory due to the above described problems. The potential higher resolution of beam imaging with lenses versus the pinhole is not exploited due to the high noise level and low beam intensity.

The original idea of equipping the new beam port with CVD diamond windows in order to take profit of less scattering and higher transmission of low energies proves during operation to be complicated owing to the high photon flux. Ozone production in air is unavoidable, leading to strong corrosion on all surrounding equipment, and the heat load on the lenses is – without being above the damage level – important.

If the problems related to the high photon flux can be resolved, this beam port will be available also for other diagnostics in future. Mainly those diagnostics that would need low X-ray energies or even visible light can profit from the CVD window.

REFERENCES

[1] F. Ewald, P. Elleaume, et al. "Vertical emittance measurement at the ESRF", DIPAC'11, Hamburg, May 2011, MOPD61.

[2] B. Lengeler, J. Tümmler, et al. "Transmission and gain of singly and doubly focusing refractive X-ray lenses", Journal of Applied Physics, 84, p. 5855 (1998).

ISBN 978-3-95450-127-4